Supporting Information

"Modeling Pyran Formation in the Molybdenum Cofactor: Protonation of Quinoxalyl-Dithiolene Promotes Pyran Cyclization"

Douglas R. Gisewhite,[†] Alexandra L. Nagelski,[†] Daniel Cummins,[‡] Glenn P. A. Yap,[‡] Sharon J. N. Burgmayer[†]*

†Department of Chemistry, Bryn Mawr College, Bryn Mawr, Pennsylvania 19010, United States

‡Department of Chemistry and Biochemistry, University of Delaware, Newark, Delaware 19716, United States

corresponding author email: sburgmay@brynmawr.edu

Contents:

Figure S1. ^{1}H NMR spectrum of BMOQO in chloroform-d.

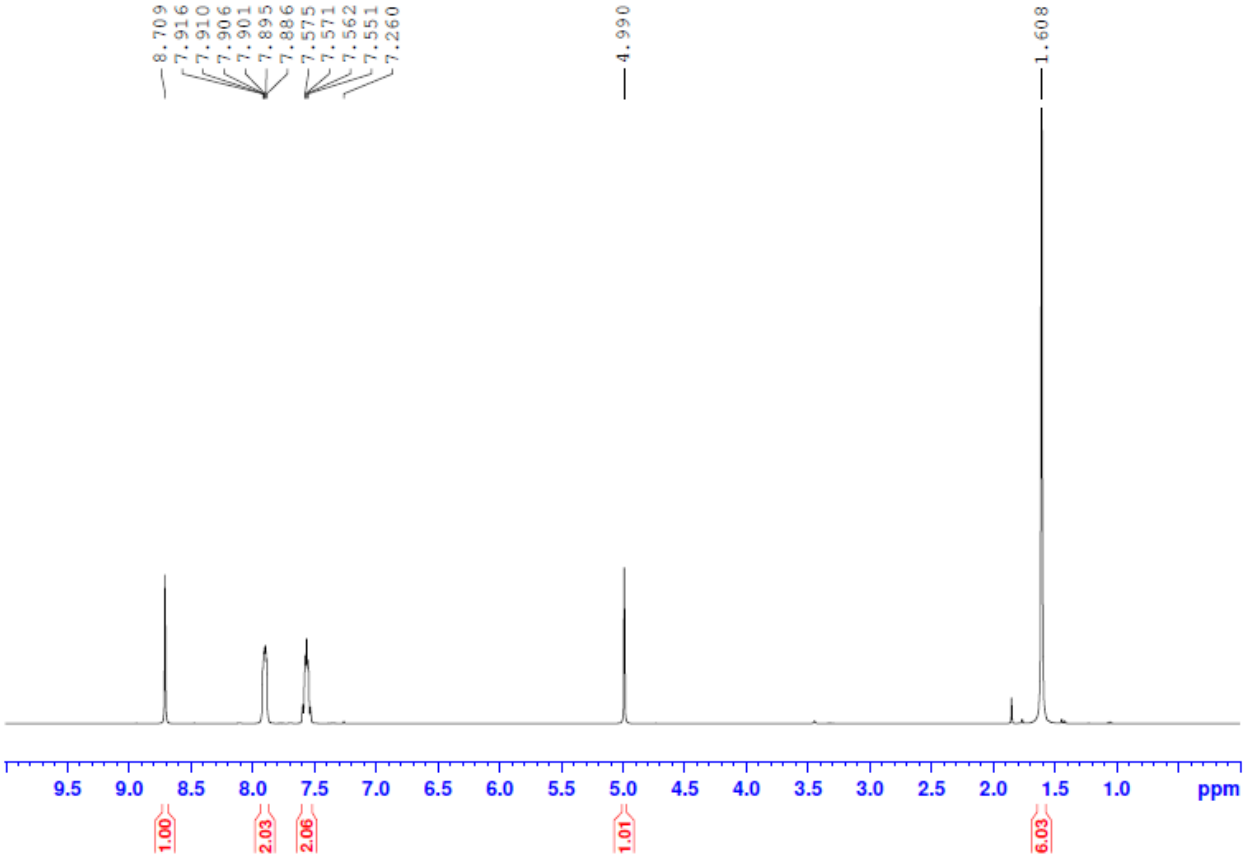

Figure S2. ^{1}H NMR spectrum of [TEA][Tp*Mo(O)(S_2BMOQO)] **2** in chloroform-d.

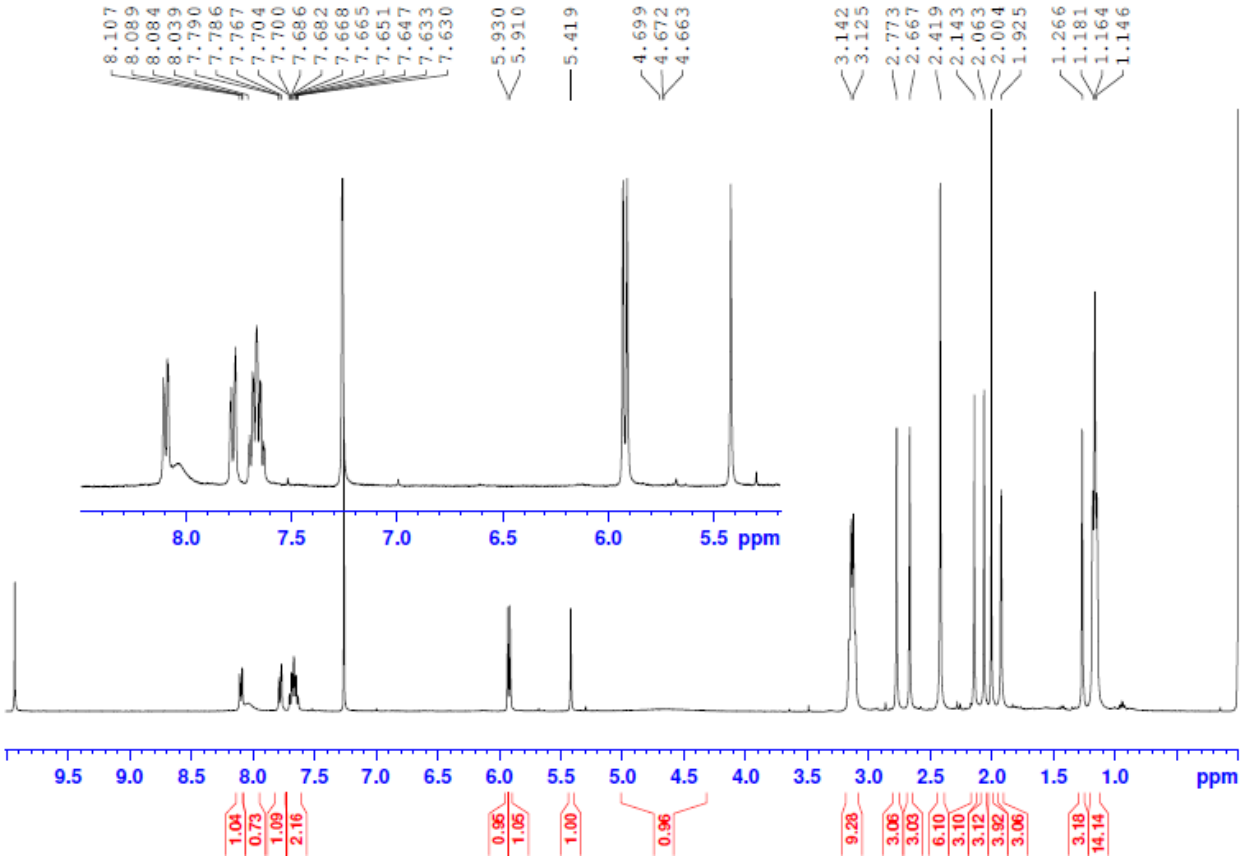

Figure S3. ^{1}H NMR spectrum of [TEA][Tp*Mo(O)(S_2BMOQO)] **2** in acetonitrile-d^3.

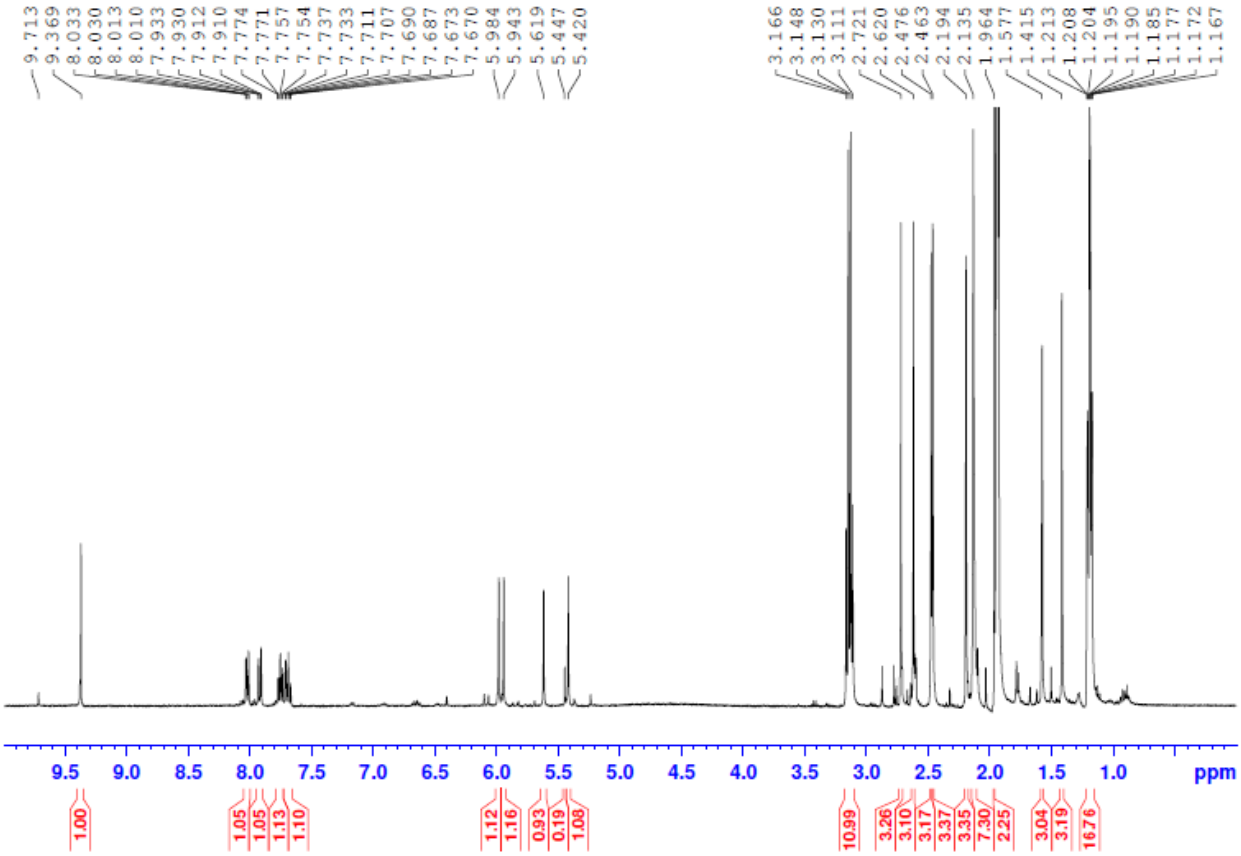

Figure S4. HSQC of [TEA][Tp*Mo(O)(S_2BMOQO)] **2** in chloroform-d.

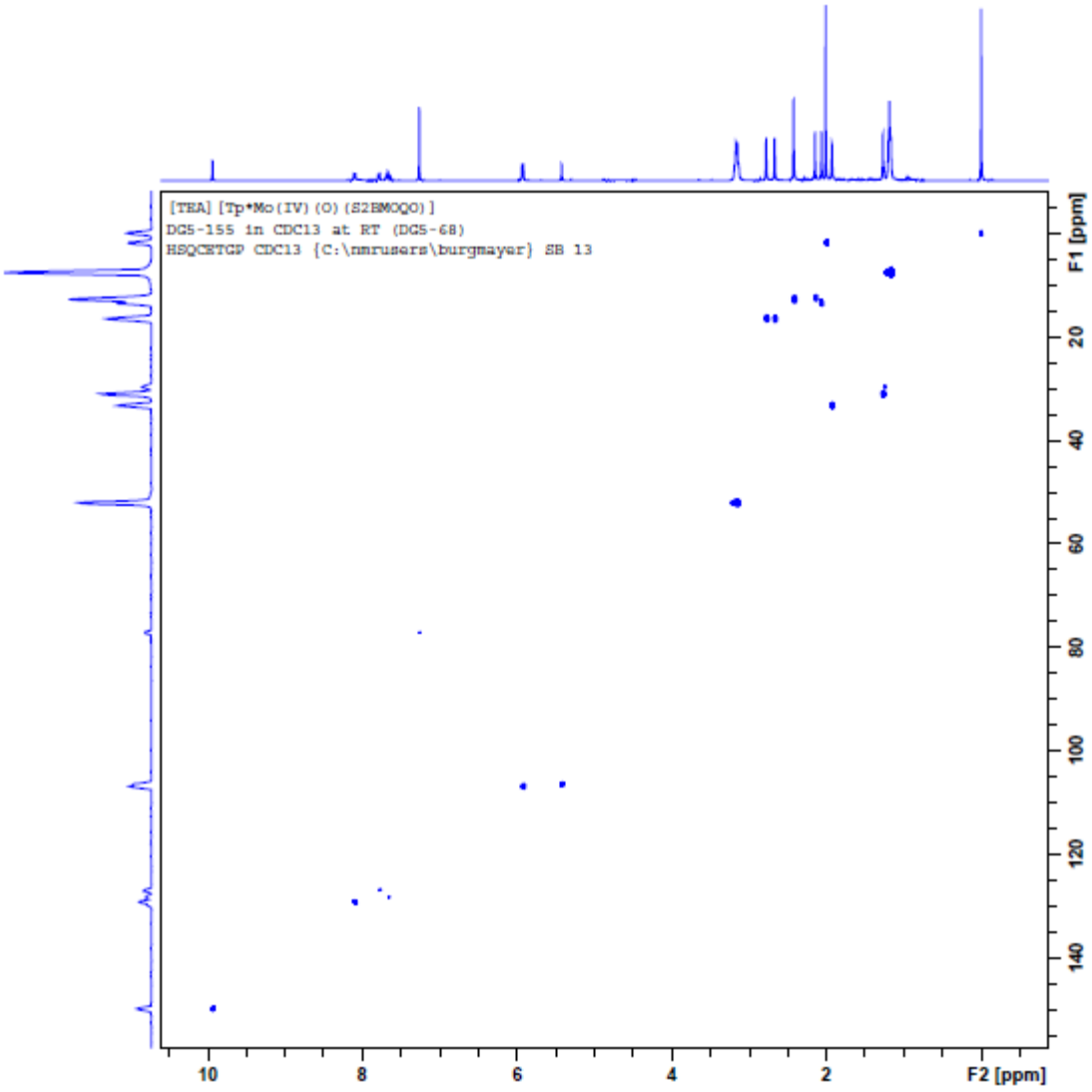

Figure S5. HSQC of [TEA][Tp*Mo(O)(S_2BMOQO)] **2** in acetonitrile-d^3.

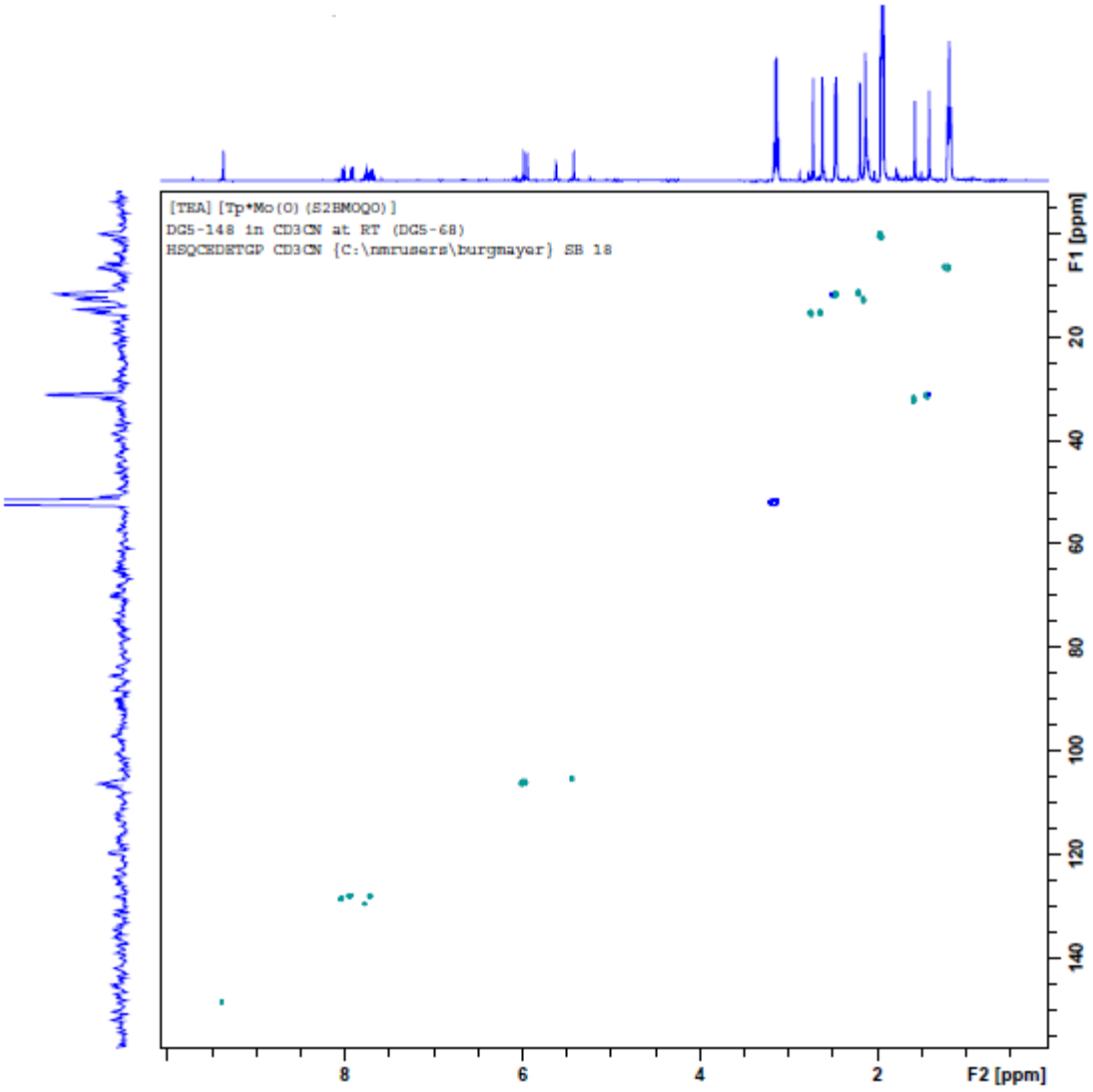

Figure S6. ^{1}H NMR spectrum of BDMQO in chloroform-d.

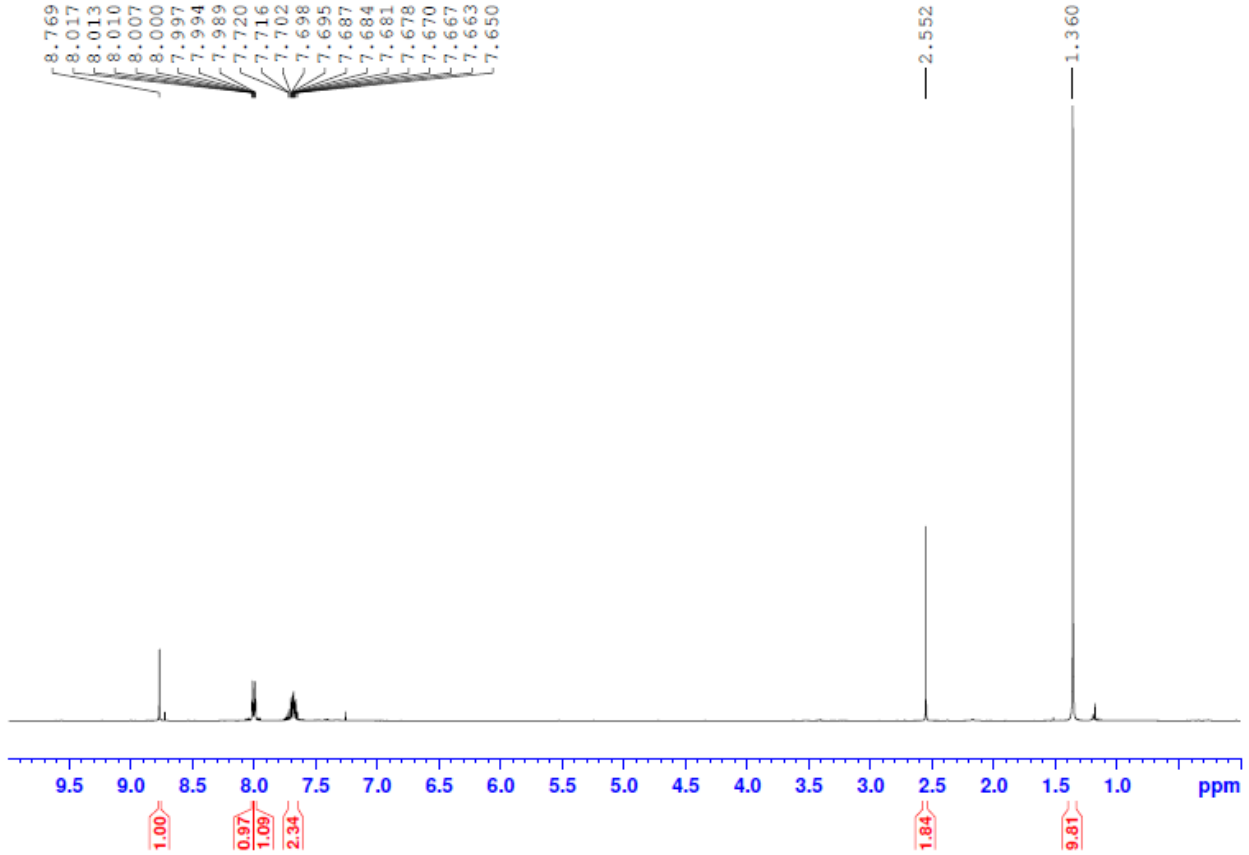

Figure S7. ^{1}H NMR spectrum of [TEA][Tp*Mo(O)(S_2BDMQO)] **4** in chloroform-d.

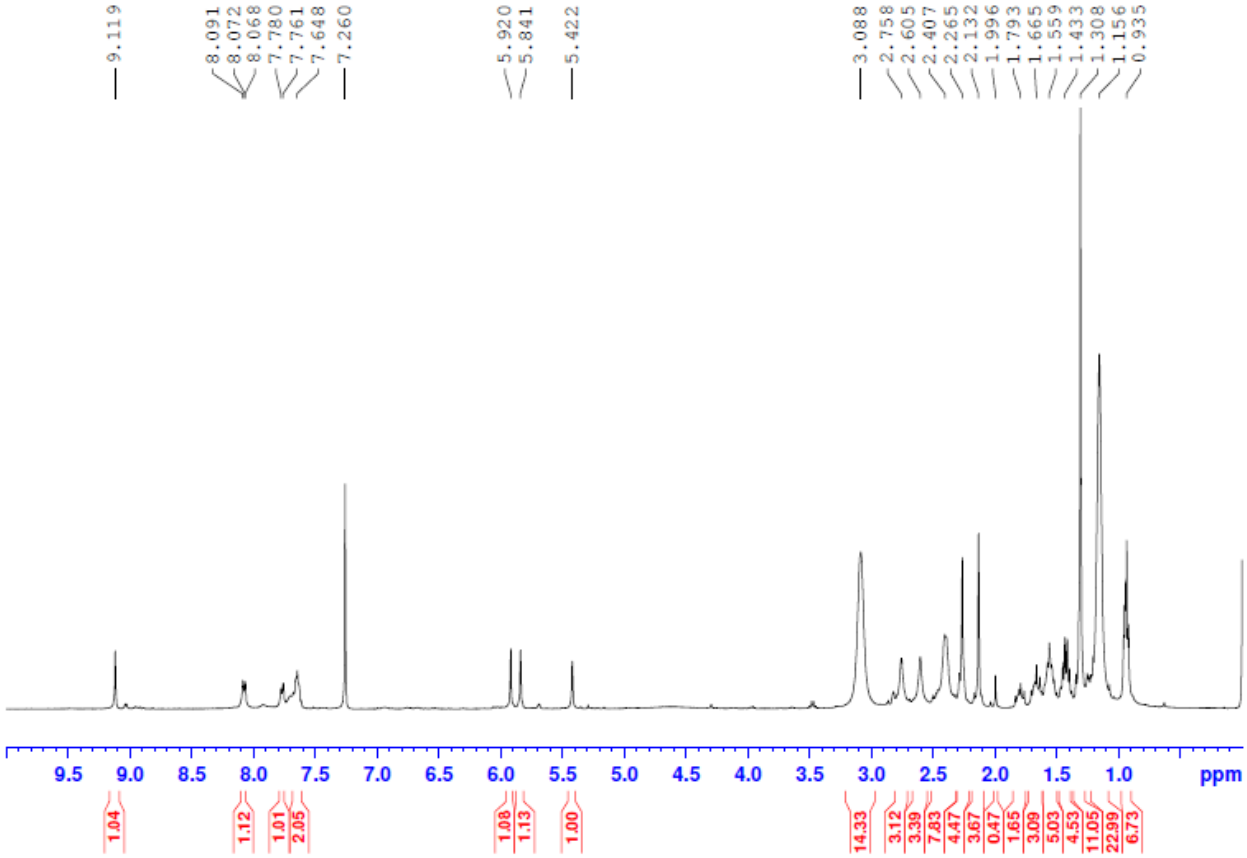

Figure S8. ^{1}H NMR spectrum of [TEA][Tp*Mo(O)(S_2BDMQO)] **4** in acetonitrile-d^3.

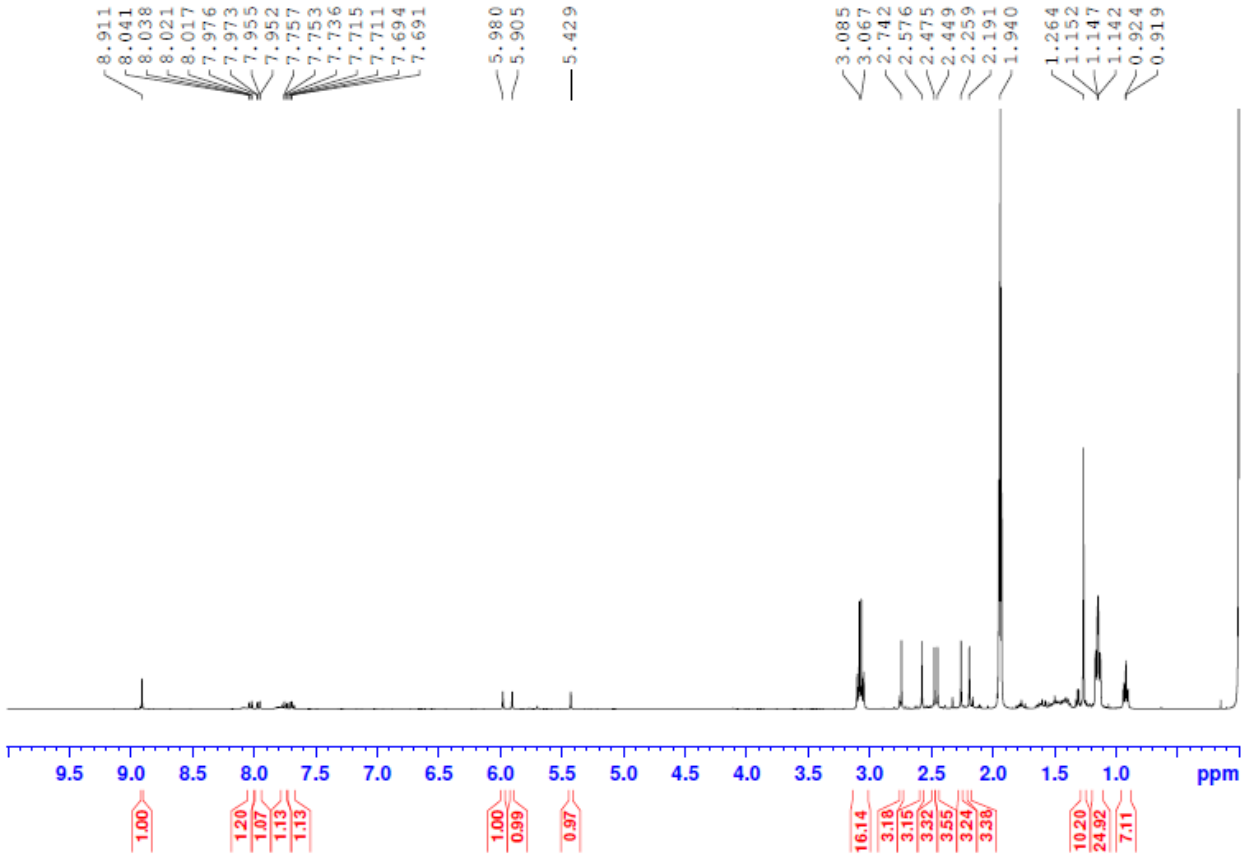

Figure S9. HSQC of [TEA][Tp*Mo(O)(S_2BDMQO)] **4** in chloroform-d.

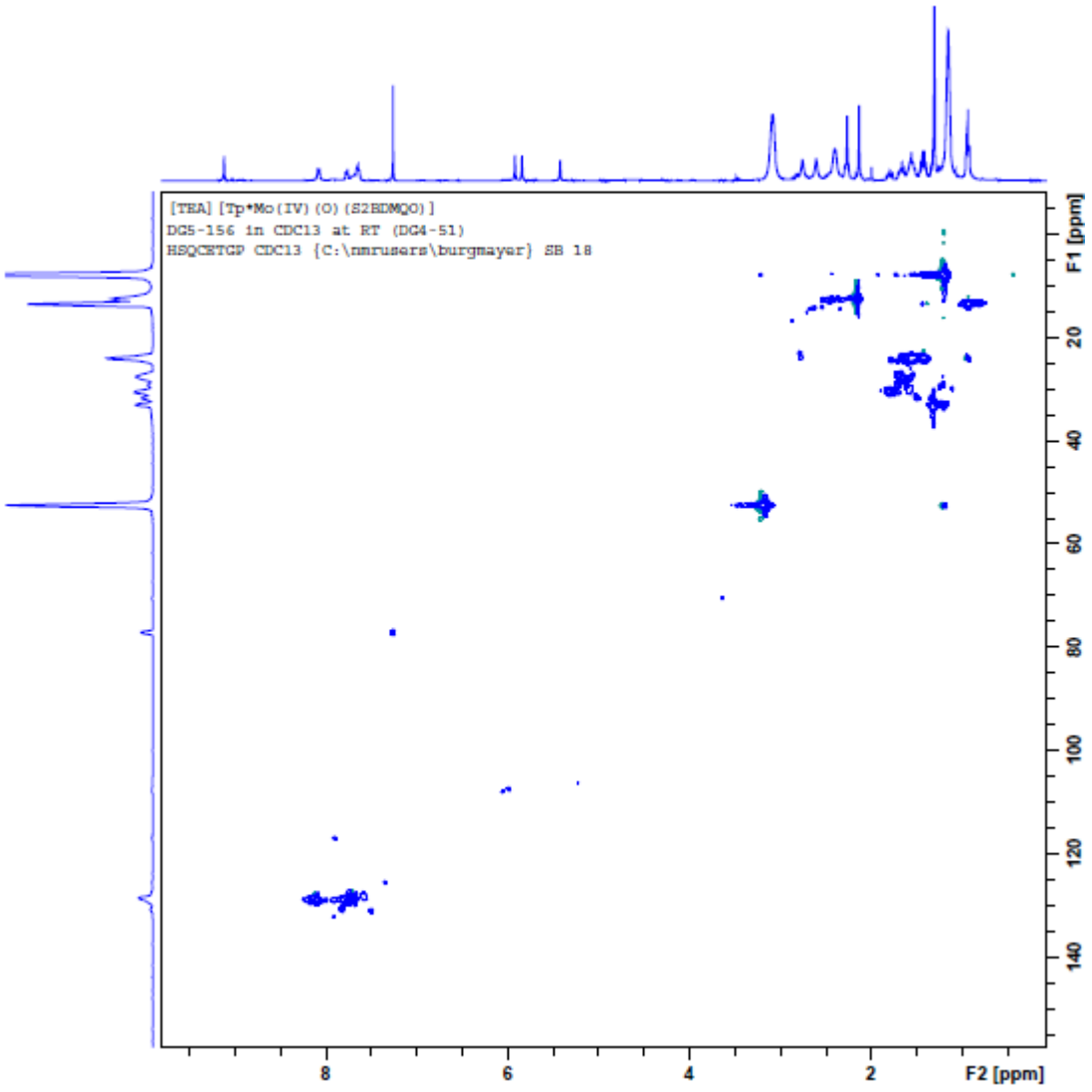

Figure S10. HSQC of [TEA][Tp*Mo(O)(S_2BDMQO)] **4** in acetonitrile-d^3.

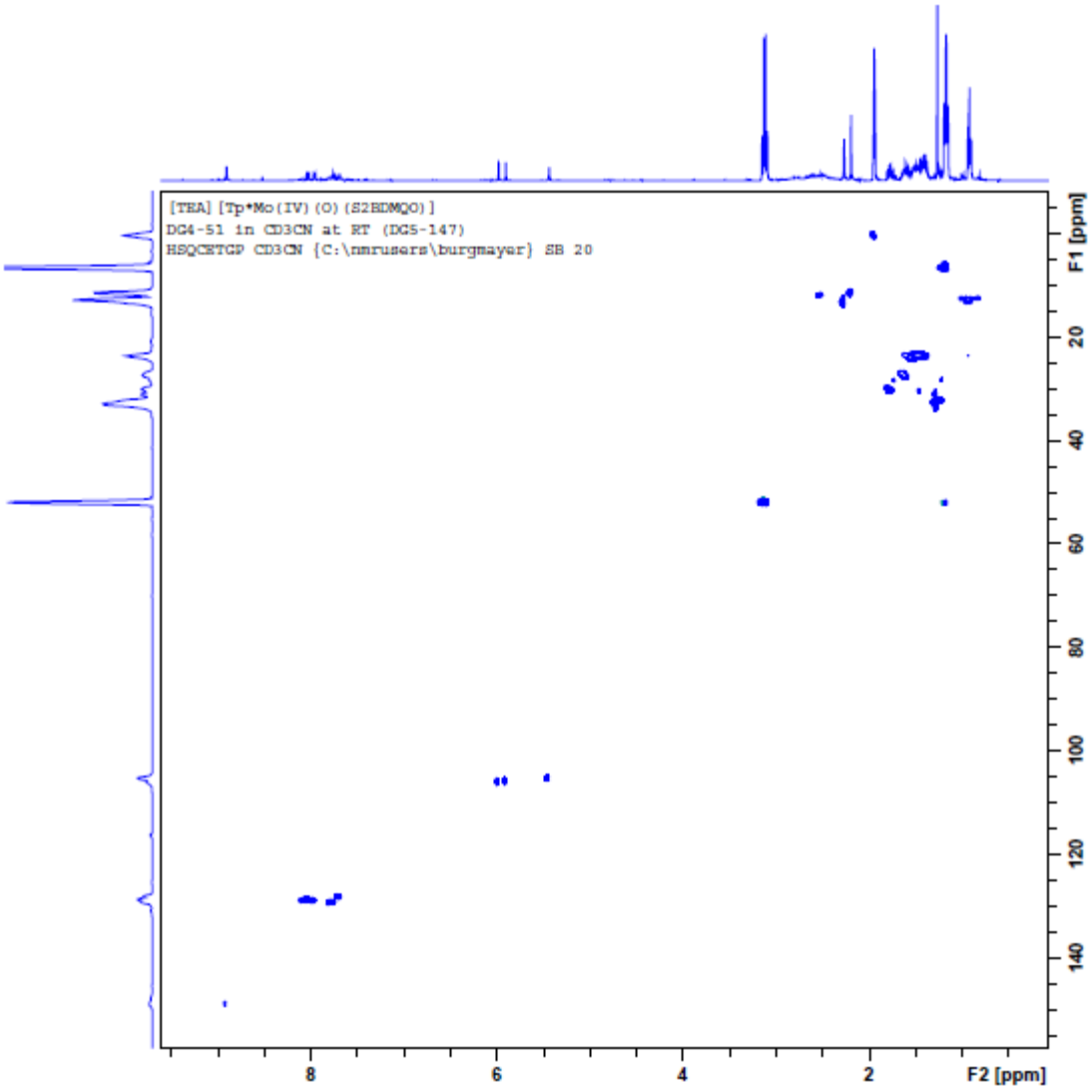

Figure S11. HSQC of Tp*Mo(O)(pyrano-H-S_2BMOQO) **7** after TFAA addition yielding pyran ring formation in acetonitrile-d^3.

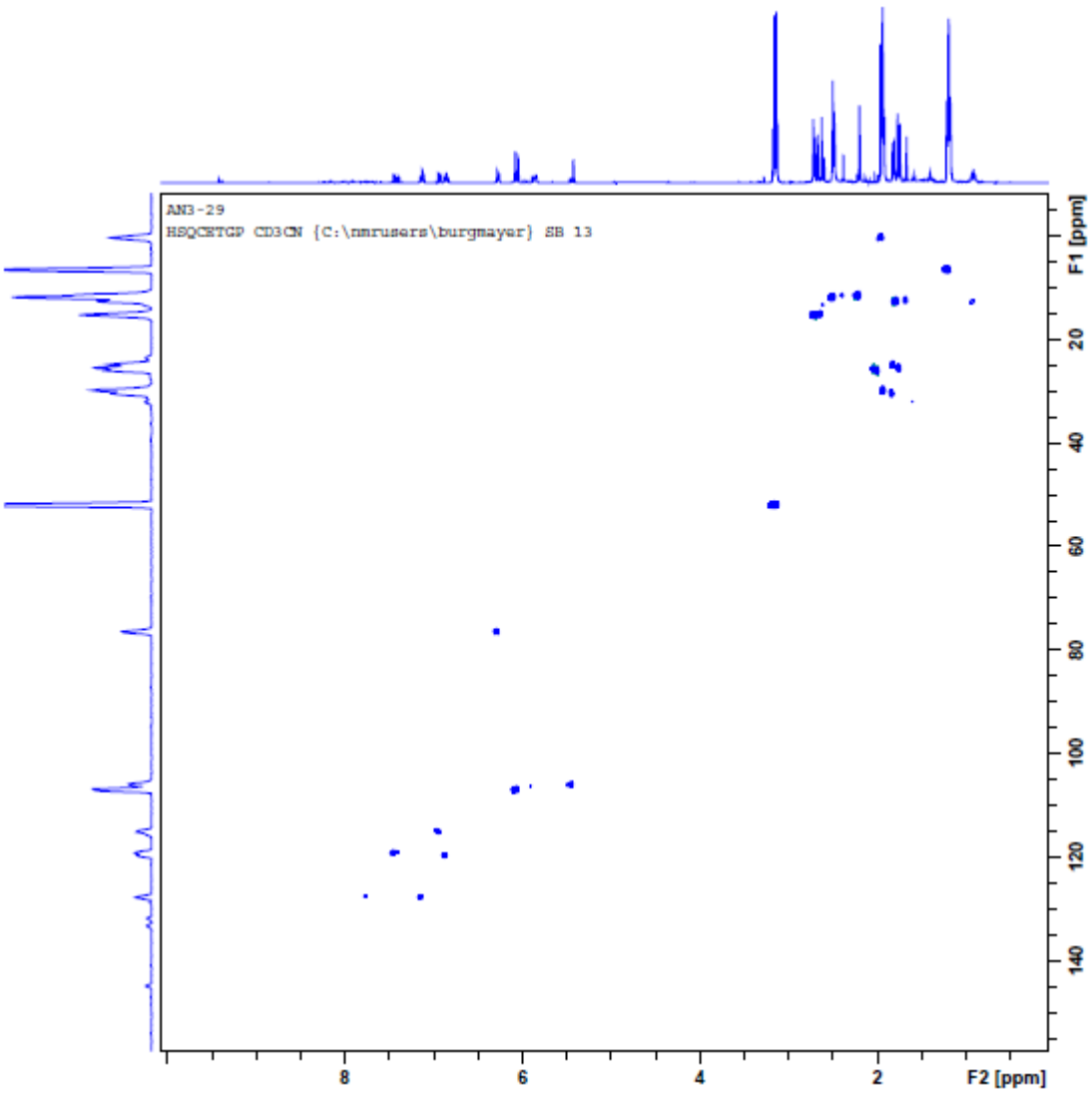

Figure S12. HSQC of Tp*Mo(O)(pyrrolo-S_2BMOQO) **8** after TFAA addition yielding pyrrole ring formation in acetonitrile-d^3.

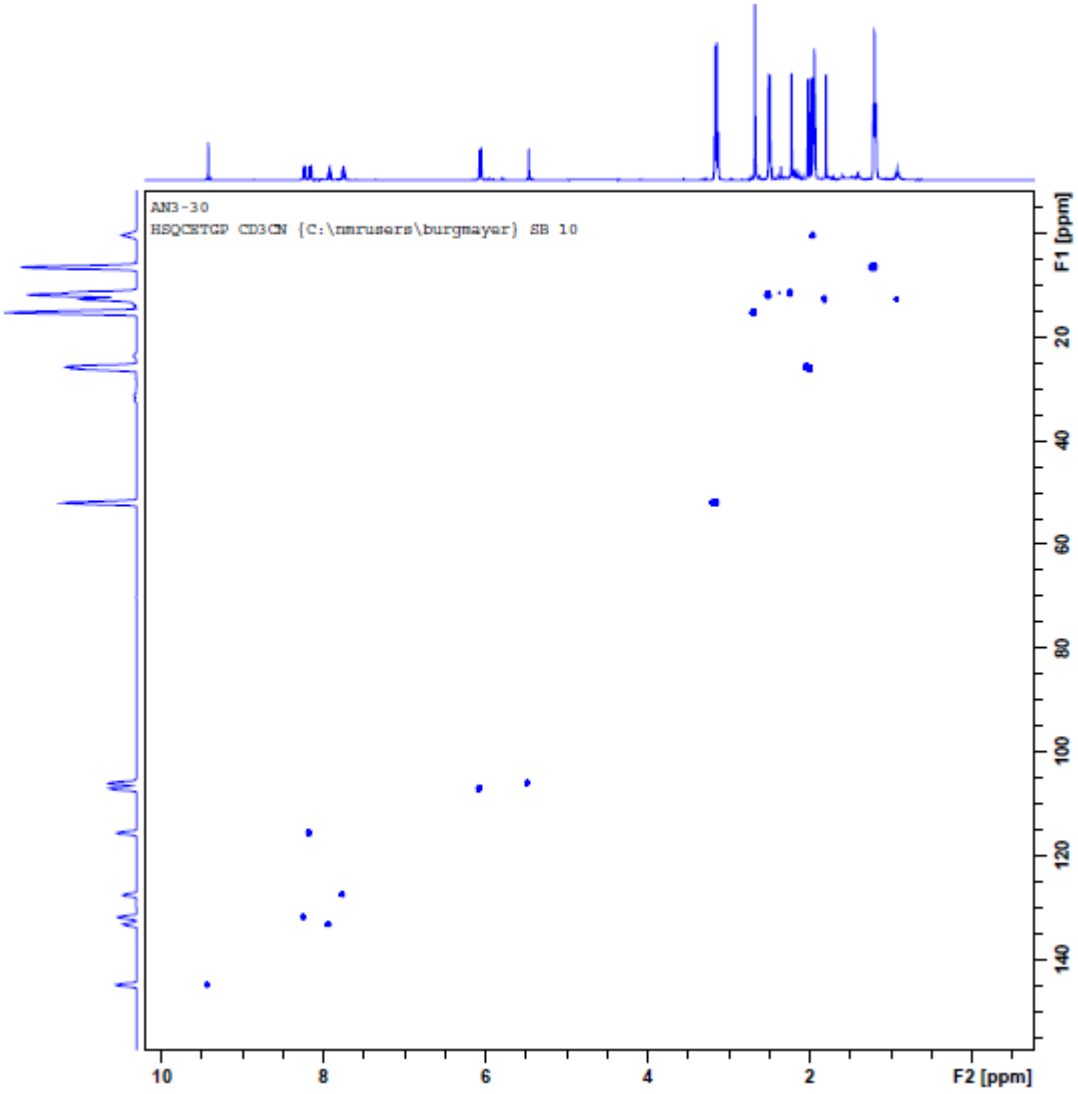

Figure S13. UV-vis overlay of **1** (blue) and **2** (red) in acetonitrile at 3.00 x 10^{-5} M.

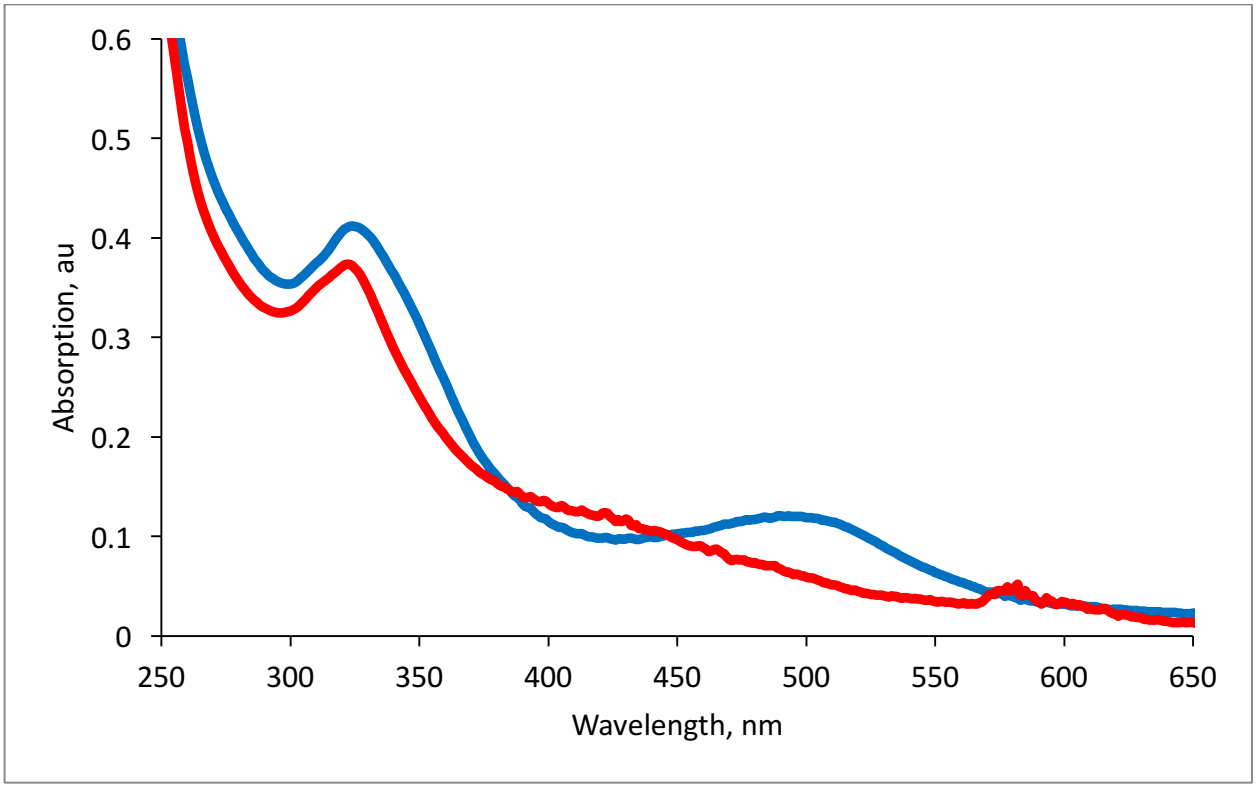

Figure S14. Cyclic voltammogram overlay of **1** (blue) and **2** (red) in acetonitrile.

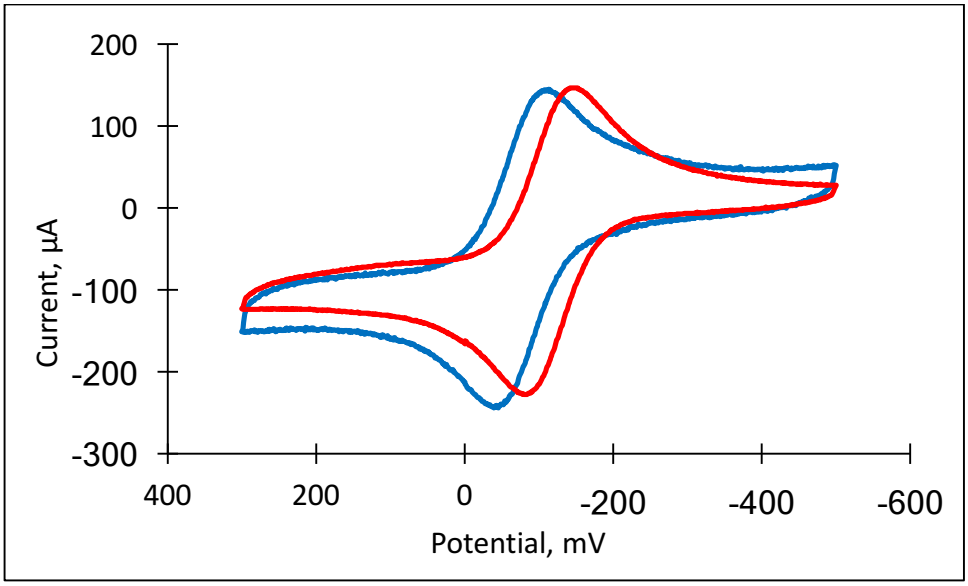

Cyclic voltammograms of the Mo^{IV}/Mo^{V} couple of **2** (blue) and **4** (red) in 0.10 M (n-Bu_4N)(ClO_4)/CH_3CN vs. Ag/AgCl at a Pt working electrode, scan rate 100 mV/s. Mo^{IV}/Mo^{V} potentials: **1** -566 mV, **2** -681 mV vs. Fc/Fc^{+}.

Table S1. Cyclic voltammometric data for **2** and **4** in acetonitrile.

Complex (solvent)	Scan rate, mV/s	E(1/2), mV [a]	$p_c - p_a$, mV [b]	i_c/i_a, [c]
2 (CH_3CN)	25	-502	75	1.04
2 (CH_3CN)	100	-503	69	1.03
2 (CH_3CN)	400	-500	63	0.99
2 (CH_3CN)	800	-500	68	1.00
Fc+/Fc (CH_3CN)	100	+429	66	1.05
4 (CH_3CN)	25	-556	69	0.95
4 (CH_3CN)	100	-552	65	1.05
4 (CH_3CN)	400	-557	61	1.06
4 (CH_3CN)	800	-557	71	1.01
Fc+/Fc (CH_3CN)	100	+438	80	1.08

[a] Fc+/Fc vs. Ag/AgCl

[b] difference between cathodic and anodic potentials

[c] ratio of cathodic to anodic currents

Figure S15. Cyclic voltammogram overlay of protonated and non-protonated forms of **2** in chloroform.

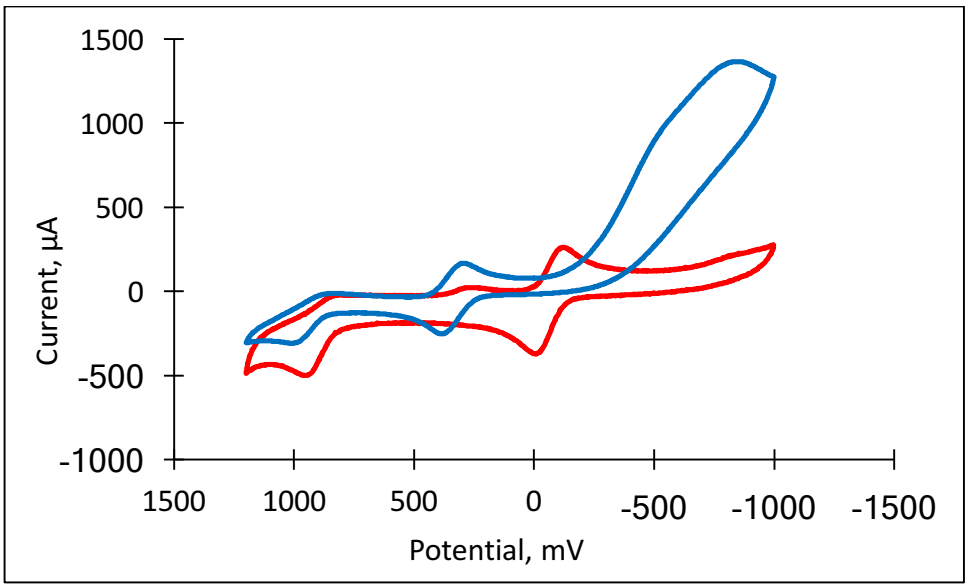

Cyclic voltammograms of the protonated form of **2** (blue) and the non-protonated form of **2** (red) in 0.10 M (n-Bu_4N)(ClO_4)/$CHCl_3$ vs. Ag/AgCl at a Pt working electrode, scan rate 100 mV/s. Mo^{IV}/Mo^{V} potentials: protonated **2** -231 mV, non-protonated **2** -566 mV vs. Fc/Fc^{+}.

Figure S16. Cyclic voltammogram overlay of protonated and non-protonated forms of **2** in acetonitrile.

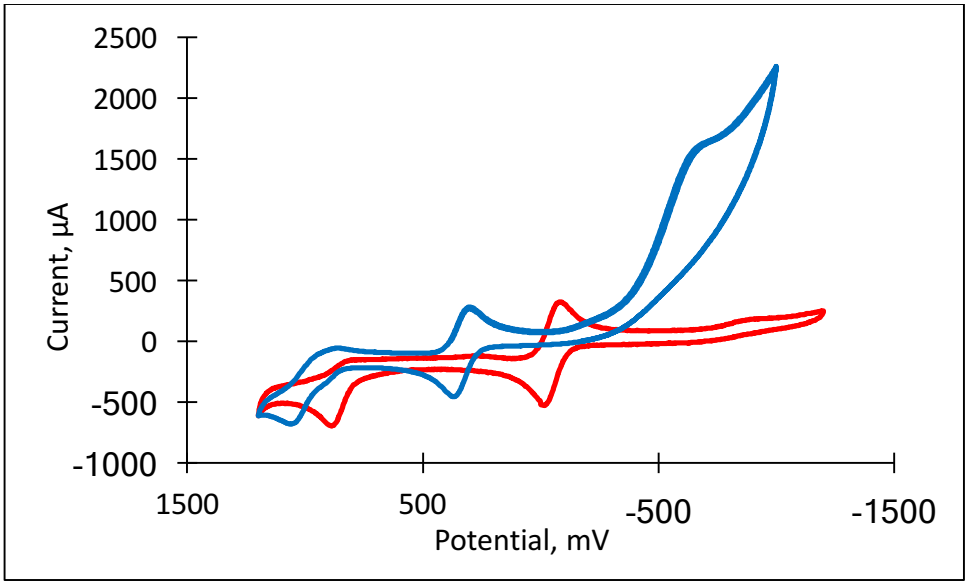

Cyclic voltammograms of the protonated form of **2** (blue) and the non-protonated form of **2** (red) in 0.10 M (n-Bu_4N)(ClO_4)/CH_3CN vs. Ag/AgCl at a Pt working electrode, scan rate 100 mV/s. Mo^{IV}/Mo^{V} potentials: protonated **2** -135 mV, non-protonated **2** -501 mV vs. Fc/Fc^{+}.

Figure S17. Cyclic voltammogram overlay of protonated and non-protonated forms of **4** in chloroform.

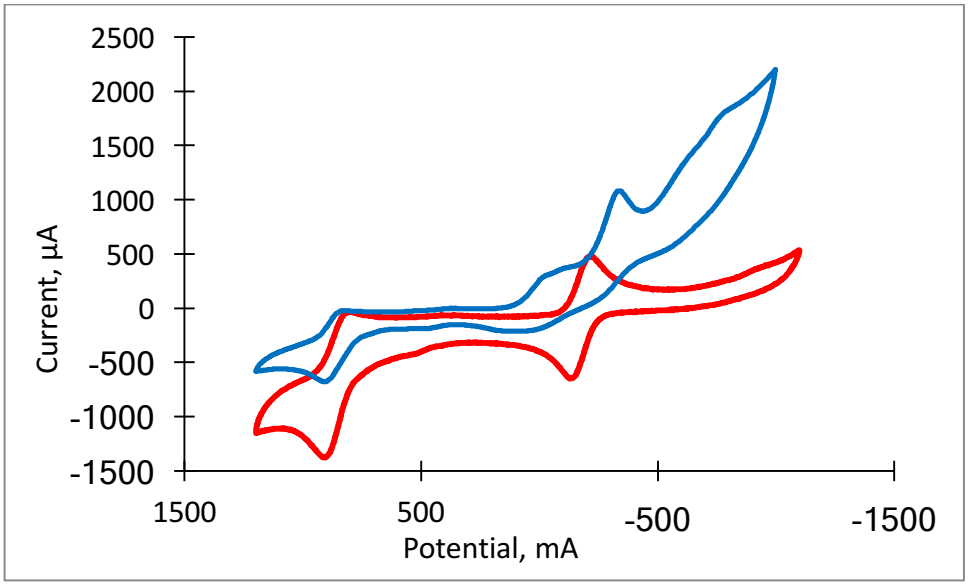

Cyclic voltammograms of the protonated form of **4** (blue) and the non-protonated form of **4** (red) in 0.10 M (n-Bu_4N)(ClO_4)/$CHCl_3$ vs. Ag/AgCl at a Pt working electrode, scan rate 100 mV/s.

Figure S18. Cyclic voltammogram overlay of protonated and non-protonated forms of **4** in acetonitrile.

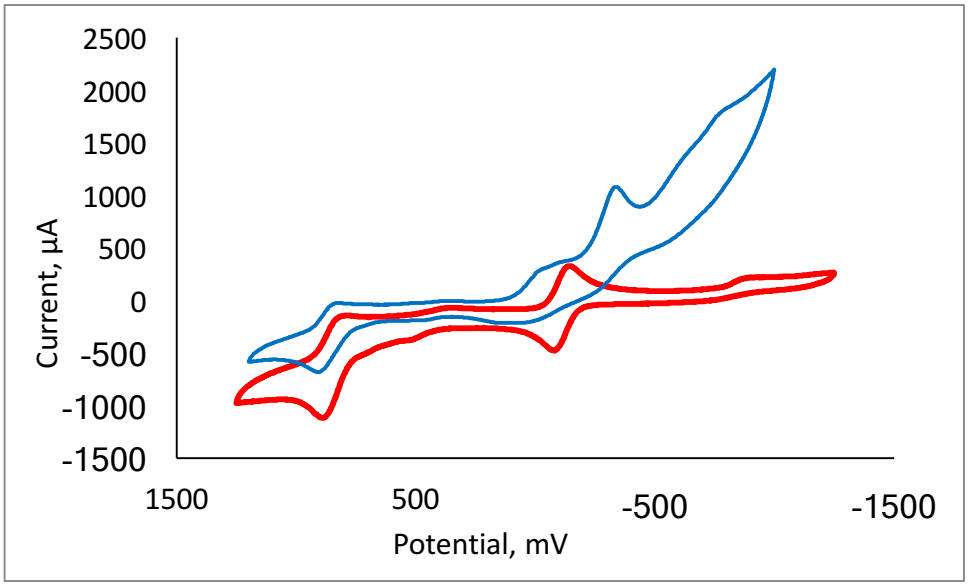

Cyclic voltammograms of the protonated form of **4** (blue) and the non-protonated form of **4** (red) in 0.10 M (n-Bu_4N)(ClO_4)/CH_3CN vs. Ag/AgCl at a Pt working electrode, scan rate 100 mV/s.

Table S1. Summary of X-ray crystal structure data for complexes **2** and **4**.

	2	**4**
Formula	$C_{38}H_{58}BCl_2MoN_9O_2S_2$	$C_{37}H_{56}BMoN_9OS_2$
Fw	914.70	813.77
Cryst Syst	Orthorhombic	Orthorhombic
space group:	Pbcn	Pbcn
a (Å)	27.8479 (14)	30.2788 (14)
b (Å)	19.8016 (10)	19.0169 (8)
c (Å)	17.9310 (9)	18.1264 (8)
α (deg)	90	90
β (deg)	90	90
γ (deg)	90	90
V (Å^3)	9887.7 (9)	10437.3 (8)
Z	8	8
ρ_{calc} (g/cm^{-3})	1.229	1.036
T (K)	200	200
radiation, λ (Å)	0.71073	0.71073
Abs coeff (mm^{-1})	0.497	0.363
wR_2 (%)	16.02	18.08
R_1 (%)	5.38	5.46
GOF	1.033	1.025

Figure S19. UV-Vis time course study over 22 hours for reactions resulting from the protonation of **2** upon addition of 1 eq. of TFAA in $CHCl_3$**.** Red line: spectrum recorded immediately after 1 eq TFAA is added to **2** in CHCl3 corresponding to **7**. Blue line: spectrum of final product **8**.